

# **JGR** Oceans

## **RESEARCH ARTICLE**

10.1029/2025JC023093

### **Key Points:**

- Moorings at the western boundary and in the upper 3,000-m depth of the array are an essential part of the 26°N observing system
- Hydrographic sections can replace the deepest moorings along the eastern boundary and the Mid-Atlantic Ridge to reliably estimate the Atlantic Meridional Overturning Circulation (AMOC)
- A reduced RAPID array would lead to an additional error that does not compromise the accuracy of the AMOC trend and variability

#### **Supporting Information:**

Supporting Information may be found in the online version of this article.

#### Correspondence to:

T. Petit, tillys.petit@noc.ac.uk

#### Citation:

Petit, T., Smeed, D., Blaker, A., Elipot, S., Johns, W., Kajtar, J. B., et al. (2025). Evaluation of a reduced RAPID array for measuring the AMOC. *Journal of Geophysical Research: Oceans*, 130, e2025JC023093. https://doi.org/10.1029/2025JC023093

Received 27 JUN 2025 Accepted 23 OCT 2025

## **Author Contributions:**

A. Blaker, J. B. Kajtar

Methodology: T. Petit, D. Smeed,
S. Elipot

Visualization: T. Petit

Writing – original draft: T. Petit

Writing – review & editing: T. Petit,
D. Smeed, A. Blaker, S. Elipot, W. Johns,
J. B. Kajtar, D. Rayner, B. Sinha,
R. H. Smith, D. L. Volkov, B. Moat

Conceptualization: D. Smeed, B. Moat

Investigation: T. Petit, D. Smeed,

© 2025. The Author(s). This is an open access article under the terms of the Creative Commons Attribution License, which permits use, distribution and reproduction in any medium, provided the original work is properly cited.

# **Evaluation of a Reduced RAPID Array for Measuring the AMOC**

T. Petit<sup>1</sup>, D. Smeed<sup>1</sup>, A. Blaker<sup>1</sup>, S. Elipot<sup>2</sup>, W. Johns<sup>2</sup>, J. B. Kajtar<sup>1</sup>, D. Rayner<sup>1</sup>, B. Sinha<sup>1</sup>, R. H. Smith<sup>3</sup>, D. L. Volkov<sup>3</sup>, and B. Moat<sup>1</sup>

<sup>1</sup>National Oceanography Centre, Southampton, UK, <sup>2</sup>Rosenstiel School of Marine, Atmospheric, and Earth Science, University of Miami, Miami, FL, USA, <sup>3</sup>Atlantic Oceanographic and Meteorological Laboratory, NOAA, Miami, FL, USA

**Abstract** Observation-based estimates of the Atlantic Meridional Overturning Circulation (AMOC) and meridional heat transport (MHT) are necessary to better understand their evolution in the coming years. The RAPID-MOCHA-WBTS array at 26°N is the only trans-Atlantic observing system to provide 20+ years of continuous measurements of the AMOC and MHT. While the design of the array has continuously evolved as our understanding of the AMOC has advanced, and as new technologies have become available, a new goal is to design a lower-cost and more sustainable observing system to continue AMOC estimations with high accuracy. Using the RAPID array data and ocean reanalyzes, we evaluate the error in the AMOC estimate due to the choice of data included in its calculation. We find that the trend and variability of the volume transport in the upper 3,000-m of the water column are not captured with sufficient accuracy by synoptic hydrographic data or ocean reanalyzes. However, moorings in the deep ocean interior along the eastern boundary and the Mid-Atlantic ridge can be replaced by hydrographic data from repeat trans-Atlantic hydrographic sections to reliably estimate the AMOC trend and variability. Experiments simulating the observing system in a high-resolution ocean model further show that the additional error in the long-term AMOC estimate induced by the substitution of mooring measurements below 3,000-m depth at these locations is small (0.30 Sv) as compared to the AMOC uncertainty.

**Plain Language Summary** An observing system at 26°N across the North Atlantic, called the RAPID-MOCHA-WBTS array, has been designed to observe and understand changes in the Atlantic Meridional Overturning Circulation (AMOC) over time. After more than 20 years of observations, a goal is now to redesign the array into a less expensive and more sustainable observing system to keep monitoring the AMOC in the future. We show that moorings localized below 3,000-m depth on each side of the Mid-Atlantic ridge and at the eastern boundary of the array could be replaced by data from repeat trans-Atlantic hydrographic sections without losing accuracy in the AMOC estimate and without modifying the AMOC trend or its uncertainty. However, the risk of using ocean reanalysis or hydrographic data instead of moorings at the western boundary or in the upper 3,000-m depth at the eastern boundary is unacceptably high, meaning that the moorings at these locations and depths are an essential part of the 26°N observing system.

## 1. Introduction

The Atlantic Meridional Overturning Circulation (AMOC) is a system of currents that play a key role in the climate system by redistributing heat, salt and carbon through the Atlantic Ocean. By carrying 60%–90% of the total heat and freshwater transports (Johns et al., 2011; McDonagh et al., 2015; Talley, 2003; Tooth et al., 2024), variations in the AMOC strength can lead to profound environmental, social and economic impacts (Bellomo et al., 2021; Zhang et al., 2019). The Intergovernmental Panel for Climate Change (IPCC AR6) projects that the AMOC will very likely decline in the 21st century due to the impacts of anthropogenic greenhouse gas emissions (Bellomo et al., 2021; Fox-Kemper et al., 2023), but the timescale and magnitude of decline remains unclear due to challenges in accurately representing the AMOC in climate models. It is thus essential to maintain robust and continuous observations of AMOC strength, which can serve as a benchmark for numerical models.

Observations have shown that seasonal and shorter-term variability can alias estimates of the AMOC from sparse hydrographic surveys (Kanzow et al., 2009), which highlights the need for making continuous measurements on the ocean boundaries with moorings (Kanzow et al., 2010). Since April 2004, the RAPID-MOCHA-WBTS array at 26°N (hereafter referred to as the RAPID array) has delivered the longest time series of the AMOC from direct observations. The 20-year timeseries has revealed substantial AMOC variability across 10-day to decadal

timescales, much of it driven by fluctuations in the atmospheric wind patterns (Zhao & Johns, 2014). Subsequently, the OSNAP array was deployed at higher latitudes in April 2014 (Lozier et al., 2019). The two arrays have demonstrated, among other findings, large AMOC variability and an apparent disconnect between the two AMOC timeseries at subannual timescales (Frajka-Williams et al., 2023; Jackson et al., 2022). The disconnect between subpolar and subtropical AMOC suggests large variations in the AMOC across latitudes, although the short overlapping period of the observing arrays limits the conclusions that can be drawn about AMOC connectivity on longer timescales. An ongoing challenge of the AMOC observing systems is thus to continue measuring the AMOC at high accuracy while using cost-effective and sustainable designs and methodologies to allow AMOC monitoring on interannual to decadal timescales.

Initially composed of 19 moorings covering the western boundary, eastern boundary and mid-Atlantic ridge of the 26°N transect, the design of the RAPID array has evolved over the years as our understanding of the AMOC has advanced, and as new technologies have become available (McCarthy et al., 2015). The desire to reduce cost and to increase sustainability prompts us to explore other observation methods and array designs. Indeed, measurements at high frequency might not be needed at all mooring locations as the impact of hydrographic fluctuations on the AMOC depends on the local magnitude of the variability (McCarthy et al., 2017). For example, hydrographic variability is weaker at depth than at the surface, suggesting that infrequent data can be used at depth whilst maintaining reasonable accuracy of the AMOC estimate. Thus, the goal of this study is to investigate to what extent moored instruments from the RAPID array at 26°N can be replaced by data from other sources, while preserving the accuracy of the RAPID AMOC estimate.

## 2. Materials and Methods

#### 2.1. The RAPID Array

The RAPID array is supported by three coordinated research programs: RAPID funded by UK Natural Environment Research Council, the Meridional Overturning Circulation Heatflux Array (MOCHA) funded by the US National Science Foundation, and the Western Boundary Time Series (WBTS) project funded by the US National Oceanic and Atmospheric Administration. Transport across the array is estimated by combining (a) transports measured by a subsea electromagnetic cable in the Florida Straits (Meinen et al., 2010; Volkov et al., 2024), (b) Ekman transports estimated from reanalysis wind stress (Hersbach et al., 2020), (c) transports estimated from direct velocity measurements at the western boundary wedge, and (d) internal geostrophic transports estimated from a mooring array stretching from the Bahamas to the Canary Islands (McCarthy et al., 2015). The RAPID array yields a basin wide transport profile T and an associated overturning streamfunction  $\Psi$  in depth space at a 12-hourly timescale,  $\Psi(t,z) = \int T(t,z) dz$ , with the AMOC strength estimated as the maximum of the overturning streamfunction. The RAPID array also provides meridional heat transport and freshwater transport across the array. For more details on their calculation and uncertainties, see Johns et al. (2023) and McDonagh et al. (2015).

The moorings deployed along the western and eastern slopes of the basin are designed to measure water properties at specific depths using moored-CTD (Conductivity-Temperature-Depth) instruments. The data from separate moorings are concatenated to create boundary temperature and salinity profiles, which are used in the estimation of the internal geostrophic transport (Section 2.2). The choice of separate moorings used in the calculation has evolved over time due to technical issues or technological developments (Figure S1 in Supporting Information S1). For example, internal geostrophic transport was estimated from three moorings at the western boundary (WB), two moorings at the Mid-Atlantic Ridge (MAR), and five moorings at the eastern boundary (EB) during its first deployment in 2004 (Cunningham et al., 2007). However, only mooring WB3 was used along the WB from November 2005 to March 2006 due to the failure of WB2 during this period. Later, the moorings initially deployed on each side of the MAR and at depths greater than 3,000-m (EB1 and EBHi) along the EB were removed in December 2020. Currently, only the data from three moorings at the WB (WB2, WBH2 and WB3) and three moorings at the EB (EBH1, EBH2, EBH3) are now used in the estimation of internal geostrophic transport (Figure 1). In this study, we evaluate the impact of the array changes made in 2020 on the AMOC estimation and investigate potential future adjustments.

## 2.2. Estimation of Internal Geostrophic Transport

The estimation of internal geostrophic transport at the RAPID array is based on geostrophic balance:

PETIT ET AL. 2 of 14

nlinelibrary.wiley.com/doi/10.1029/2025/C023093 by NICE, National Institute for Health and Care Excellence, Wiley Online Library on [27/11/2025]. See the Terms and Condi

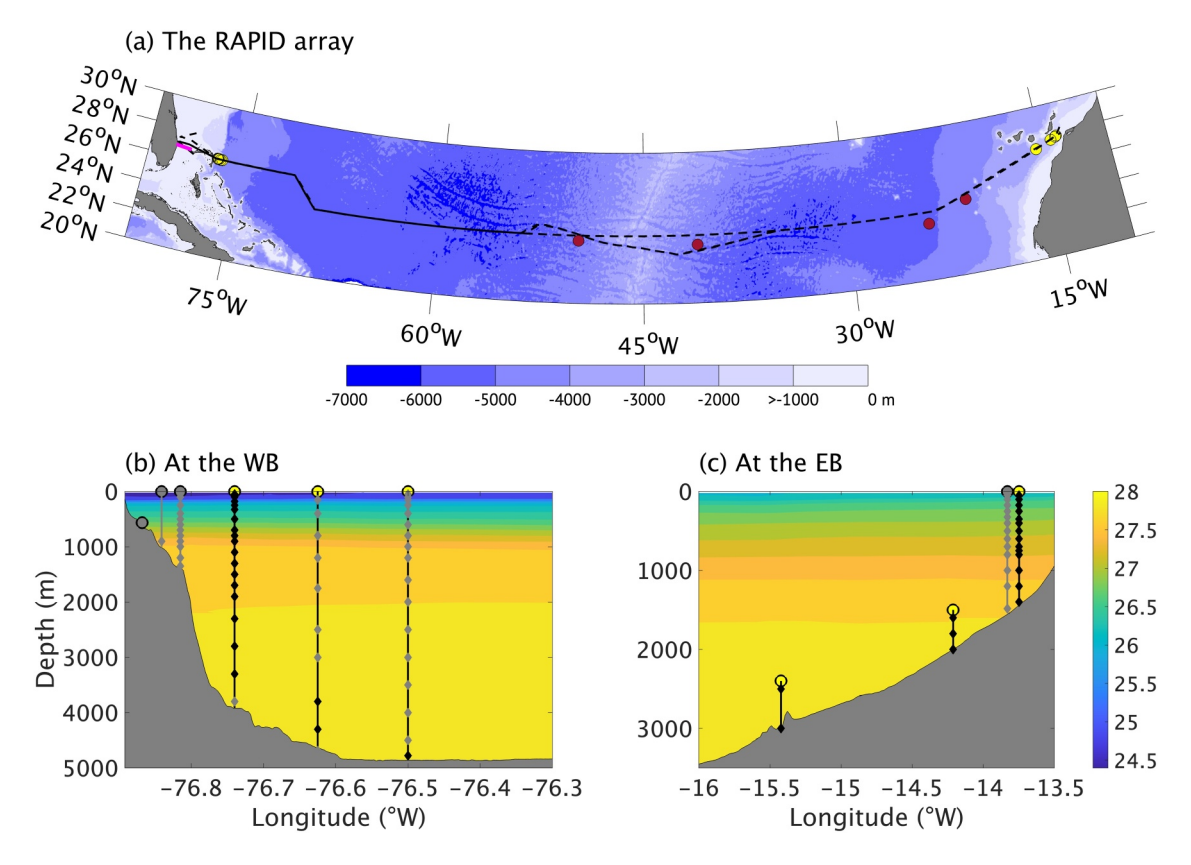


Figure 1. The RAPID array since December 2020. (a) Location of the current moorings (yellow dots), the moorings removed in December 2020 (red dots), the Florida Straits cable (purple line) and the A05 hydrographic sections (black dashed lines) shown with ETOPO1 bathymetry. (b, c) Mean density from the four A05 sections with mooring locations along (b) the western boundary (from left to right: WBadcp, WB0, WB1, WB2, WBH2, WB3) and (c) the eastern boundary (from left to right: EBH1, EBH2, EBH3, EBH3\_backup). Dots on moorings indicate the location of moored CTD instruments. Moorings and sensors in light gray are not used in the calculation of the internal geostrophic transport.

$$\frac{\partial p}{\partial x} = \rho f v,\tag{1}$$

with  $\frac{\partial p}{\partial x}$  the zonal pressure gradient,  $\rho$  the density of sea water, f the Coriolis parameter, and v the northward velocity. Beal and Bryden (1999) showed that this balance can be applied over the full depth range with high accuracy and even within strong boundary currents. The vertical profile of pressure, relative to a reference level  $P_r$ , is related to the dynamic height  $\phi$  along each boundary:

$$\phi(P) = -g \int_{P_{\sigma}}^{P} \delta \, dP,\tag{2}$$

where g is the gravitational acceleration and  $\delta$  is the specific volume anomaly. The internal geostrophic transport  $T_{\rm int}$  (m<sup>2</sup>/s) between two hydrographic profiles can thus be calculated following Equation 3:

$$T_{\rm int}(P) = \frac{1}{f} \left( \phi_{\rm East}(P) - \phi_{\rm West}(P) \right). \tag{3}$$

Within the RAPID methodology, the reference level of  $T_{\rm int}$  is chosen to be 4,820 db, or the bottom where it is shallower, and the transport at the reference level is determined by a requirement that the net meridional volume transport is zero (see McCarthy et al. (2015) for full details).

PETIT ET AL. 3 of 14

The accuracy of the AMOC estimate from the RAPID array has been assessed by previous studies. McCarthy et al. (2015) showed that the uncertainty of the 10-day AMOC estimation is 1.5 Sv when combining the accuracy of the moored instruments (0.002°C for temperature, 0.003 psu for salinity and 1 db for pressure) with systemic uncertainty estimates in the other components of the total transport (Kanzow et al., 2010). Considering structural factors of the array, Sinha et al. (2018) showed from a high-resolution model that the mean overturning streamfunction can be biased by factors that include the choice of a single reference level, regions not sampled by the array (i.e., bottom triangles), and unaccounted ageostrophic motions. The model suggests that these sources of uncertainties, which are common to other mooring-based arrays in the Atlantic (Frajka-Williams et al., 2023), may introduce a bias of ~1.2 Sv for the 5-day AMOC estimation at RAPID.

## 2.3. Error in the AMOC Estimate Due To Changes in the Array Design

We evaluate the impact of substituting portions of the mooring array for other observation-based data (i.e., hydrographic data or ocean reanalyzes) for the AMOC. Following the method described above, a dynamic height profile of a given data is estimated from temperature and salinity profiles selected as close as possible to the mooring locations. The dynamic height profile is subsampled onto the vertical grid of the mooring-based profile and linearly interpolated in time to match the temporal sampling of the RAPID timeseries. Finally, the boundary profile constructed in this way, from the given data, is used to replace all or part (e.g., deeper than a specified depth) of the mooring-based profile at a specified boundary.

The error in the monthly-averaged estimation of the AMOC due to the choice of data used in its estimation is evaluated by calculating the difference between (1) the AMOC estimates made from full mooring measurements and (2) the AMOC estimates made when some of the mooring data is replaced by a given data at specified depths and locations. The AMOC difference ( $\varepsilon$ ) is estimated as case (2) minus case (1) and is evaluated from April 2004 to December 2020 to exclude the effects of changes made to the mooring array in December 2020. The temporal mean and standard deviation of the AMOC difference respectively represent the bias,  $\overline{\varepsilon(t)}$ , and random error,  $\sqrt{\text{Var}[\varepsilon(t)]}$ , where the overbar denotes a time average and Var [.] is the variance operator. The total AMOC error due to the choice of data used in its estimation is then characterized by the root mean square error:

$$RMSE = \sqrt{\overline{\varepsilon(t)}^2 + Var[\varepsilon(t)]}.$$
 (4)

A primary goal of the RAPID array is to measure the multi-year trend of the AMOC and to determine whether the AMOC slowdown predicted by climate models is underway. Then, in addition to evaluating the total AMOC error that primarily represents differences in the short-term variability, it is also important to assess how the different array configurations will affect the estimation of the multi-year trend of the AMOC. The linear trend of the AMOC is estimated by applying a least squares method on the monthly AMOC estimates after removing the seasonal cycle. The uncertainty of the trend is quantified using the 95% confidence intervals. The AMOC trend and its uncertainty is  $-0.6 \pm 0.8$  Sv/decade when using the full mooring measurements (i.e., over the period April 2004 to December 2020). This estimation differs from the AMOC trend of  $-0.8 \pm 0.7$  Sv/decade recently estimated by Volkov et al. (2024) because the AMOC trend and its uncertainty are particularly impacted by the length of the AMOC timeseries used for its estimation (Figure S2 in Supporting Information S1), which covers a shorter time period in our analysis (2004–2020 instead of 2004–2022), while the impact of time resolution between the timeseries (monthly instead of 10-day) is lower.

#### 2.4. The Hydrographic Sections A05 and WBTS

We assessed the use of the hydrographic sections A05 and WBTS in replacement of portions of the RAPID mooring array. We used four GO-SHIP A05 sections (Atkinson et al., 2012; Fu et al., 2018) that were made at ~26°N between 2004 and 2020 (Figure 1a). The hydrographic sections were carried out from 4 April to 10 May 2004 (124 profiles), 6 January to 18 February 2010 (135 profiles), 6 December 2015 to 22 January 2016 (145 profiles), and 19 January to 1 March 2020 (134 profiles). The vertical resolution of the profiles is 2 dbar, and the separation distance between the profiles is between 50 and 80 km in the ocean interior, and less than 20 km along the western continental slope.

PETIT ET AL. 4 of 14

The WBTS sections sample the western boundary once every 9 months, approximately, with a total of 28 sections between 2001 and 2023 (Chomiak et al., 2022). The vertical and horizontal resolutions of the profiles are 1 dbar and 20 km over the RAPID mooring locations, respectively.

Boundary profiles were constructed using a combination of at least 5 CTD stations around each mooring location to reduce the eddy signal in the infrequent CTD data. To achieve this for the A05 data, we selected temperature and salinity profiles within  $3^{\circ}$  of the mooring locations at the EB,  $1^{\circ}$  of the mooring locations at the MAR, and  $0.25^{\circ}$  of the mooring locations at the WB. For the WBTS data, we selected temperature and salinity profiles within  $0.5^{\circ}$  of longitude of the mooring locations at the WB.

## 2.5. Ocean Reanalyzes

Although numerous ocean reanalyzes are available (Balmaseda et al., 2015), we restricted our choice to those that continuously and publicly update their timeseries, an important consideration for maintaining up-to-date estimates of the AMOC. The two gridded ocean reanalyzes used to test substituting portions of the RAPID mooring array are the monthly ocean reanalysis EN4.2.1 (Good et al., 2013) and the monthly NEMO model-based product GLORYS12 (Lellouche et al., 2021). EN4.2.1, called EN4 here, has a horizontal resolution of 1° and 42 depth levels. It is derived from objective analysis of Argo profiling floats and other profile data from the World Ocean Database. GLORYS12 has a finer 1/12° horizontal resolution and 50 depth levels. It assimilates along track altimeter sea-surface height, sea-surface temperature as well as in situ temperature and salinity profiles.

#### 2.6. The High-Resolution Ocean Model RAPID36

RAPID36 is based on NEMO v4.2.2 (Madec et al., 2023) with the SI3 ice model (Vancoppenolle et al., 2023). The configuration is similar to the global 1/4° configuration of GOSI9, the NOC/UK Met Office configuration developed under the Joint Marine Modeling Program (Guiavarc'h et al., 2025). A two-level AGRIF nest is implemented in the subtropical North Atlantic with a horizontal grid refined to 1/12° over the latitude range 9–42°N, and further refined to 1/36° over 19–31°N. In all cases the vertical grid has 75 levels with an increasing layer thickness from 1 m at the surface to a maximum of 250 m at the bottom, and partial steps representing the bottom topography. The simulation is forced by surface meteorological conditions based on the Japanese Meteorological Agency Reanalysis JRA55-do (Tsujino et al., 2018), which is highly correlated with ERA5, and spans the period 1976–2023. Here, monthly model outputs are analyzed during the period January 1990 to December 2023.

The AMOC in the model is calculated following the RAPID methodology as closely as possible (Sinha et al., 2018). The mid-ocean geostrophic transport is calculated from dynamic heights at the virtual mooring positions with a reference depth of 5,090 m. Slightly different from the real-world configuration, the virtual moorings are situated along a single quasi-zonal grid line at ~26°N and include only one WB mooring extending from the seafloor to surface at 76.58°W, MAR moorings at 49.67°W and 40.33°W, and EB moorings at 22.06, 15.47, 15.17, 14.94, and 14.50°W. Transports across the Florida Straits and Western Boundary Wedge are computed directly from model prognostic velocities, and time-invariant AABW transport is computed from the mean (1990–2023) velocities below the reference depth. Finally, Ekman transport is calculated from the model zonal wind stress, which is derived from JRA55-do.

The model agrees favorably with the RAPID observations in several diagnostics (Figure S3 in Supporting Information S1). In particular, the correlation between the modeled and observed AMOC timeseries is strong, at  $0.69 \ (p < 0.01)$ , although the modeled AMOC (13.9 Sv) is 3 Sv (18%) weaker than the observed AMOC (16.9 Sv) on the mean during the 2004–2022 period. This discrepancy is mainly explained by a weaker Florida Strait transport, and therefore it does not impact our analysis that focuses on changes in the design of the interior mooring array.

The model is used to quantify the level of error in the AMOC estimation introduced with the use of A05 hydrographic profiles, which exhibit limited temporal sampling (i.e., in different months and seasons) and varied spatial sampling (i.e., in different positions of the CTD profiles) from one realization to the next. Following a Monte Carlo method, numerous realizations of simulated hydrographic profiles are computed with randomized temporal and spatial sampling. Given that the A05 sections are carried out at approximately 5-year intervals, the model temperature and salinity are sampled every 5 years with a randomized shift of  $\pm 24$  months in time. Over

PETIT ET AL. 5 of 14

the 34-year analysis period (1990–2023), this yields 7 temporal data samples for each variable, which are extracted at the virtual mooring positions below 3,000-m depth along the EB and the MAR and are linearly interpolated in time for each month. The procedure is repeated to produce an ensemble of 100 timeseries, or realizations, each with random temporal shifts.

To account for the varied spatial sampling of the A05 data, we apply a uniform sampling of the modeled temperature and salinity (N sample points) over varying ranges around the mooring positions ( $\Delta$  zonal span). The data from the N points are then averaged at each depth and used to construct the profile at the virtual mooring location. We use spatial ranges of  $\Delta = 1^{\circ}$ ,  $2^{\circ}$ ,  $3^{\circ}$ ,  $4^{\circ}$ ,  $5^{\circ}$ ,  $6^{\circ}$  with N = 9 sample points for the EB and spatial ranges of  $\Delta = 0.5^{\circ}$ ,  $1^{\circ}$ ,  $1.5^{\circ}$ ,  $2^{\circ}$ ,  $3^{\circ}$ ,  $4^{\circ}$  with N = 5 sample points for the MAR, choices that are guided by the typical number of CTD profiles used in the observation-based analysis. The final AMOC error is based on the differences between the 100 realizations of modeled AMOC estimate.

## 3. Errors in the AMOC Estimate Due To a Reduced Array

The error in the AMOC estimate due to the choice of substituted data at the RAPID array is evaluated when hydrographic sections or ocean reanalyzes replace portions of the mooring array at the EB, on each flank of the MAR, and at the WB separately. We first focus on the deepest part (below 3,000-m depth) of the boundary profiles at the MAR and the EB to evaluate the error due to the substitution of the deep moorings that were removed in December 2020. Then, we investigate the error due to the substitution of other moorings at the EB and WB.

#### 3.1. Mid-Atlantic Ridge

We examine the effect of substituting the mooring-based profile of dynamic height below 3,000-m depth at the MAR for one estimated from the A05 sections, the EN4 reanalysis or the GLORYS12 model. Note that the internal geostrophic transport is computed using data from 3,700-m depth to the ocean floor on either side of the ridge.

Substituting mooring measurements for these alternative data at the MAR leads to overall small AMOC errors (Figure 2b and Table 1). The small negative bias estimated when using EN4 or A05 is explained by a full-depth underestimation of the overturning streamfunctions, while the small positive bias estimated when using GLORYS12 is explained by a full-depth overestimation of the overturning streamfunction (Figure 2a). The maximum of these transport differences is reached at ~4,000-m depth, which is close to the top of the MAR, but the transport differences are smaller at the depth of the maximum of the overturning streamfunction (i.e., at about 1,000-m depth). The random error in the AMOC estimate is also small for each substitution, although GLORYS12 introduces larger variability in the AMOC estimate (~1 Sv peak to peak) than EN4 or A05 (~0.1 Sv peak to peak). The total errors resulting from the bias and random error in the AMOC estimate are particularly small when using A05 or EN4.

More importantly, the AMOC trend and its uncertainty are not impacted by the substitution of these mooring measurements when using A05 or EN4. Using GLORYS12 leads to a slightly weaker AMOC trend during the 2004–2020 period, although the difference in the AMOC trends is less than the trend uncertainty.

## 3.2. Eastern Boundary

We next examine the effect of substituting the mooring-based profile of dynamic height below 3,000-m depth at the EB for one estimated from A05, EN4 or GLORYS12. Here, the mooring-based profile below 3,000-m depth consists of the combination of profiles from two deep moorings (EBHi and EB1) that were initially deployed along the EB but removed in December 2020 (red dots in Figure 1a).

Substituting the deep EB for A05 or EN4 leads to smaller AMOC errors than when using GLORYS12 (Figures 2c and 2d, Table 1). The error time series estimated when using GLORYS12 exhibit decadal oscillations with values larger than 1 Sv in 2006. The associated random error (0.33 Sv) leads to a total error (0.35 Sv) that can be considered as non negligible, although it is less than the uncertainty of the AMOC estimate (1.5 Sv). On the contrary, the bias and random errors in the AMOC estimates when using the sparse hydrographic measurements A05 are 0.24 Sv smaller than when using GLORYS12, leading to a total error of 0.11 Sv. Similarly, the AMOC

PETIT ET AL. 6 of 14

21699291, 2025, 11, Downloaded from https://agupubs.onlinelibrary.wiley.com/doi/10.1029/2025/C023093 by NICE, National Institute for Health and Care Excellence, Wiley Online Library on [27/11/2025]. See the Term

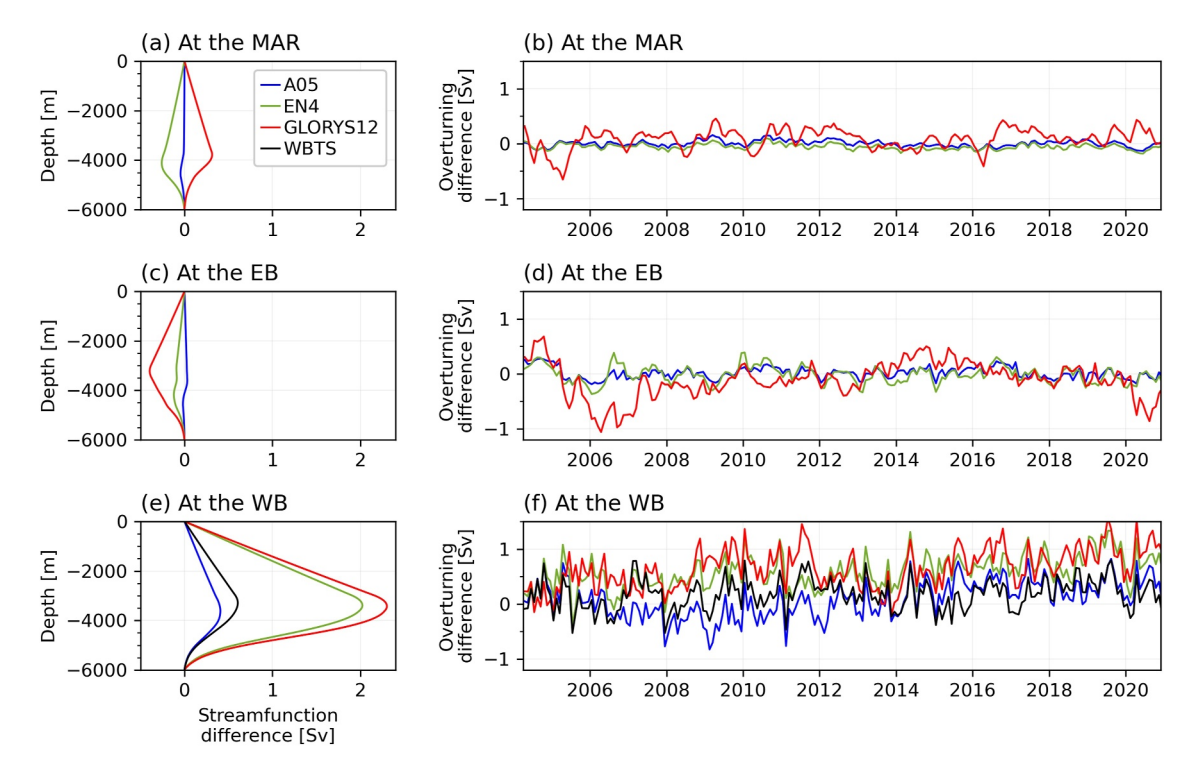


**Figure 2.** Errors induced by various products when substituting data at the RAPID array below 3,000-m depth. Differences in panels (a, c, e) overturning streamfunctions and (b, d, f) AMOC estimated when the mooring-based profiles of dynamic height deeper than 3,000-m depth are substituted for profiles estimated from the A05 sections, the WBTS sections, the EN4 reanalysis and the model-based reanalysis GLORYS12 over (a, b) each side of the MAR, (c, d) the EB, and (e, f) the WB.

trend estimated when using GLORYS12 is 0.1 Sv/decade weaker than when using the full mooring measurements, while the AMOC trend estimated when using A05 is not impacted by the substitution.

**Table 1**Summary of the AMOC Errors and Trends Based on Figure 2

		A05	EN4	GLORYS12	WBTS
MAR	Bias	-0.001	-0.06	0.08	-
	Random Error	0.06	0.05	0.19	-
	Total Error	0.06	0.08	0.21	-
	AMOC Trend	$-0.6\pm0.8$	$-0.6\pm0.8$	$-0.5 \pm 0.8$	-
EB	Bias	0.01	-0.02	-0.11	-
	Random Error	0.11	0.15	0.33	-
	Total Error	0.11	0.15	0.35	-
	AMOC Trend	$-0.6\pm0.8$	$-0.7\pm0.8$	$-0.5 \pm 0.8$	-
WB	Bias	0.09	0.58	0.65	0.17
	Random Error	0.34	0.31	0.36	0.28
	Total Error	0.35	0.66	0.74	0.33
	AMOC Trend	$-0.3\pm0.8$	$-0.3\pm0.8$	$-0.2 \pm 0.8$	$-0.5 \pm 0.8$

*Note.* Bias, random error, and total error (Sv) in the AMOC estimates based on Figures 2b, 2d, and 2f. AMOC trends are also indicated in each case (Sv/decade). Values in bold highlight the substitutions resulting in total errors less than 20% of the AMOC accuracy and AMOC trends that compares well to the AMOC trend estimated using the full mooring measurements. Note that the AMOC trend and its uncertainty is  $-0.6 \pm 0.8$  Sv/decade when using the full mooring measurements (i.e., over the period April 2004–December 2020).

Based on this result, we investigate the sensitivity of the error due to the depth range over which the mooring-based profile is substituted at the EB. Figure 3 shows AMOC errors when the A05, EN4 or GLORYS12 are used to substitute the mooring-based profile of dynamic height (1) from bottom to 3,000-m depth (same as shown in Figure 2d), (2) from bottom to 2,000-m depth, (3) from bottom to 1,000-m depth, and (4) from bottom to surface.

Compared with case (1) discussed above, substituting the EB profiles over larger depth ranges lead to significantly larger AMOC errors for each product (Figure 3 and Table 2). This is explained by greater transport differences at depths closer to the maximum of the overturning streamfunction that leads to large biases and random errors in the AMOC estimates. Then, the total errors in the AMOC estimate increase with the depth range over which the mooring-based profile is substituted and reach values that are larger than the 1.5 Sv of AMOC uncertainty when the full mooring profile is substituted. A substitution of the profile below 2,000-m depth leads to total errors that can be considered large, although it is less than the uncertainty range of the AMOC estimate. In addition, we show that the AMOC trend is significantly impacted by these substitutions, with positive AMOC trends induced when EN4 is used to replace the EB profile at depths shallower than 2,000 m.

## 3.3. Western Boundary

The mooring-based profile of dynamic height at the WB is now substituted below 3,000-m depth for those estimated from the A05 sections, the WBTS sections, the EN4 reanalysis, or the GLORYS12 model. The difference in the

PETIT ET AL. 7 of 14

21699291, 2025, 11, Downloaded from https://agupubs.onlinelibrary.wiley.com/doi/10.1029/2025JC023093 by NICE, National Institute for Health

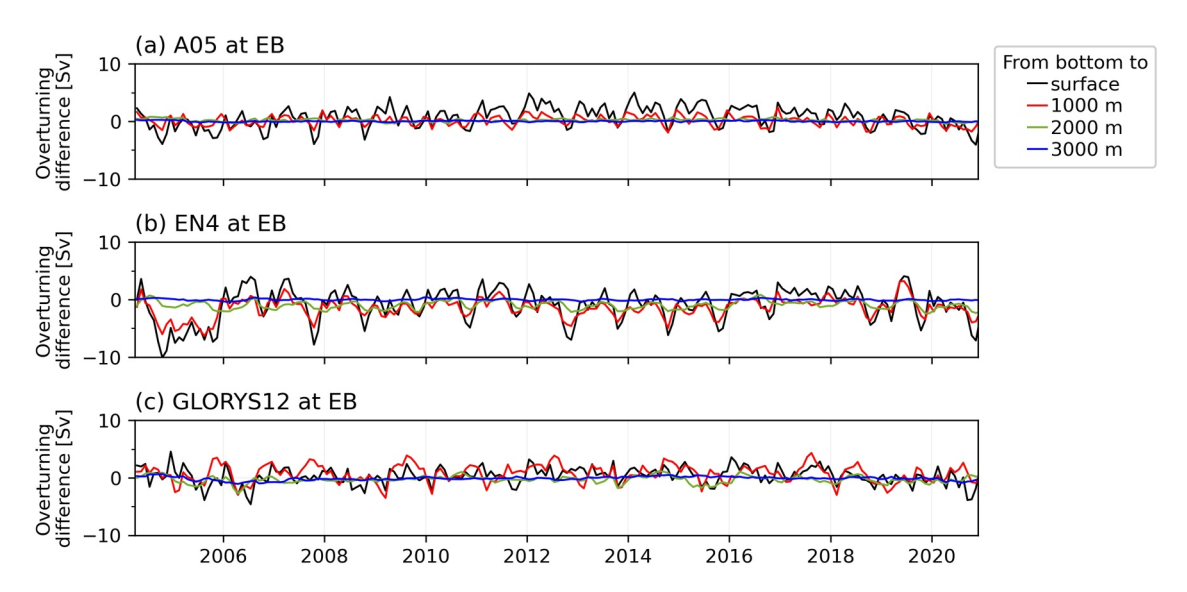


**Figure 3.** AMOC errors induced by the various product when substituting data over different depth ranges at the EB. AMOC differences estimated when the mooring-based profile of dynamic height at the EB is substituted from bottom to 3,000-m depth (blue lines), from bottom to 2,000-m depth (green lines), from bottom to 1,000-m depth (red lines), and from bottom to surface (black lines) for (a) A05, (b) EN4 or (c) GLORYS12.

mean overturning streamfunction between the two estimates is positive over the full depth range with maxima at 3,000–4,000 m (Figure 2e). In particular, the overturning streamfunction is up to 2.3 Sv stronger at 3,429 m when using GLORYS12 than when using the full mooring measurements. The large difference in overturning streamfunction at depth is explained by an increasingly stronger mean volume transport from bottom to 3,000-m depth.

Using these four products instead of the deepest part of the WB moorings leads to overall larger AMOC estimates (Figure 2f and Table 1). The associated total error is mainly driven by the bias of the AMOC estimate when using the ocean reanalysis EN4 or GLORYS12, while it is mainly driven by the random error (i.e., the monthly variability of the AMOC difference) of the AMOC estimate when using the hydrographic sections A05 or WBTS. Indeed, the AMOC error when using A05 or WBTS primarily represents the short-term variability that cannot be captured by sparse hydrographic measurements. However, using GLORYS12 or EN4 with high temporal and

 Table 2

 Summary of the AMOC Errors and Trends Induced When Substituting Data

 Over Different Depth Ranges at the EB Based on Figure 3

		Bot-2000	Bot-1000	Bot-0
A05	Bias	0.17	0.10	0.69
	Random Error	0.26	0.89	1.86
	Total Error	0.31	0.90	1.98
	AMOC Trend	$-0.7 \pm 0.8$	$-0.7 \pm 0.8$	$0.0\pm0.8$
EN4	Bias	-0.95	-1.45	-0.97
	Random Error	0.71	1.65	2.86
	Total Error	1.19	2.19	3.02
	AMOC Trend	$-0.6\pm0.8$	$0.2 \pm 0.8$	$0.5 \pm 1.0$
GLORYS12	Bias	-0.31	0.70	0.32
	Random Error	0.63	1.52	1.49
	Total Error	0.70	1.67	1.52
	AMOC Trend	$-0.6\pm0.8$	$-0.7 \pm 0.8$	$-0.6 \pm 0.8$

*Note.* Bias, random error, and total error (Sv) in the AMOC estimates based on Figure 3. AMOC trends are also indicated in each case (Sv/decade).

spatial resolutions does not lead to smaller AMOC errors than using the sparse hydrographic measurements of A05 or WBTS. In fact, the random error is about 0.3 Sv for each case and the largest total error in the AMOC estimate is found when using GLORYS12, with 0.74 Sv, which suggests that GLORYS12 does not accurately capture changes in the deep volume transport, despite its high temporal and spatial resolutions. This is possibly due to structural biases in the underlying model or in the data assimilation.

Furthermore, the positive trends in the AMOC differences suggest that the biases are non-stationary (Figure 2f). Substituting the deep WB for one of these other products leads to AMOC trends significantly weaker than the AMOC trend estimated with the full mooring measurements, although the uncertainty on these trends is not impacted (Table 1). This suggests that the deep WB moorings are needed to capture the trend in the data, while substituting the deep EB and MAR moorings for any of the products tested does not significantly impact the calculated trend.

## 4. Possible Changes in the Array Design

## 4.1. Identification of Alternative Data to Use After December 2020

We now evaluate the impact of the changes made to the RAPID array in December 2020 on the AMOC estimation, following a previous unpublished

PETIT ET AL. 8 of 14

21699291, 2025, 11, Downloaded from https://agupubs.onlinelibrary.wiley.com/doi/10.1029/2025/C023993 by NICE, National Institute for Health and Care Excellence, Wiley Online Library on [27/11/2025]. See the Terms and Conditions

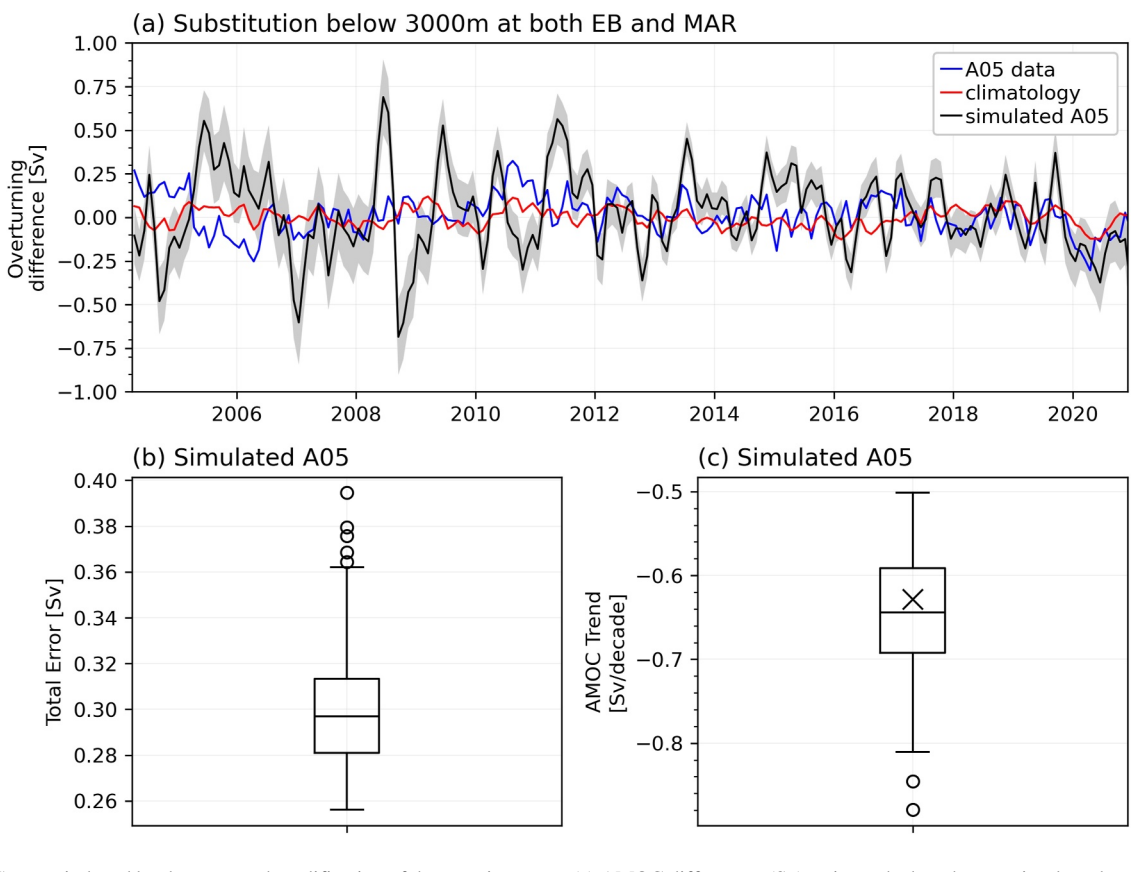


**Figure 4.** AMOC errors induced by the proposed modification of the mooring array. (a) AMOC differences (Sv) estimated when the mooring-based profiles of dynamic height at the MAR and below 3,000-m depth at the EB are replaced by profiles estimated from (red curves) their monthly climatology during 2004–2020 or (blue curves) the A05 sections. Black curves show the same as the blue curves but from the 100 numerical realizations of simulated A05 sections in the high-resolution model RAPID36. Shading area indicate one standard deviation of the 100 numerical realizations. (b) Box plot of the total error in the simulated AMOC estimate (Sv) between the 100 numerical realizations. (c) Box plot of the simulated AMOC trend (Sv/decade) in the 100 numerical realizations. The middle line indicates the median and the edges of the box indicate the first and third quartiles of the data. The whiskers indicate values within 1.5 times the interquartile range. The black cross indicates the simulated AMOC trend estimated from the original timeseries over the period 1990–2023.

analysis, and discuss potential future adjustments based on the analysis above. Since December 2020, the mooring-based profiles of dynamic height on each side of the MAR and below 3,000-m depth at the EB were replaced by profiles estimated from their monthly climatology. Figure 4a shows the difference between two AMOC estimates: the AMOC estimates made from full mooring measurements and the AMOC estimates made when the time varying dynamic height profiles at the MAR and deep EB are replaced by their monthly climatology.

Although some of the AMOC variability is lost when using monthly climatology, the bias is, as expected, negligible  $(-1.0 \times 10^{-4} \text{ Sv})$  over 2004–2020 and the random and total errors are small (0.05 Sv). The difference in the mean overturning streamfunction between the two estimates is also negligible at all depths, of the order of  $10^{-3}$  Sv. More importantly, using monthly climatology instead of these mooring data does not impact the AMOC trend or its uncertainty, which is  $-0.6 \pm 0.8$  Sv/decade. We conclude that the new design of the RAPID array implemented in December 2020 does not significantly impact the present-day AMOC estimation. It is however necessary to identify another data source that can be used in replacement of the mooring-based climatology in the future, as trends may emerge in the deep ocean temperature and salinity (McCarthy et al., 2017). It is also important to ask whether more moorings could be replaced without compromising the accuracy of the AMOC estimate at the RAPID array.

The analyses presented in Section 3 provide an estimation of error due to the substitution of moorings at the existing RAPID array. It is commonly accepted that errors less or equal to the total AMOC uncertainty can be considered as acceptable. However, it is important to note that the 1.5 Sv of AMOC uncertainty previously

PETIT ET AL. 9 of 14



## Journal of Geophysical Research: Oceans

10.1029/2025JC023093

quantified by McCarthy et al. (2015) is relatively large because it combines the accuracy of moored instruments with the systemic uncertainty estimates in other components of the total transport. Using the AMOC uncertainty as a threshold in our evaluation of the additional error due to the substitution of moorings would then leads to AMOC differences that are too large with regards to the primary goal of the RAPID array, that is to measure the multi-year trend of the AMOC and to determine whether the AMOC slowdown predicted by climate models is underway. To determine an acceptable level of error in the AMOC estimate, we require that (a) the additional error is "small" compared to the AMOC uncertainty, (b) the AMOC trend is not impacted by these substitutions, and (c) the uncertainty of the AMOC trend is not larger. Although it is difficult to objectively define a threshold under which we can consider the additional error to be "small," here we deem that errors of 20% of the total AMOC uncertainty (±0.3 Sv) and smaller can be considered as an acceptable additional error in the AMOC estimate when assessing the different array configurations.

The additional errors and AMOC trends estimated above indicate that using repeated hydrographic sections or ocean reanalysis instead of deep moorings along the WB leads to additional AMOC errors that cannot be considered as acceptable (Table 1), meaning that full moorings at the WB are necessary to continue estimating the AMOC variability and AMOC trend with the same level of accuracy. Furthermore, none of the observation-based data sets evaluated here can accurately capture the variability in the upper 3,000 m of the EB (Table 2), which reveals that the three inshore moorings at the EB (i.e., EBH1, EBH2, and EBH3) are necessary to reliably estimate the AMOC at the RAPID array. However, we show that the deep interior volume transport at the MAR and EB (below 3,000-m depth) contributes relatively little to the total AMOC across the RAPID array and can be captured by the A05 sections (Table 1 and Table S2 in Supporting Information S1). Similarly, the AMOC estimated when A05 data substitutes the deep EB and MAR data together exhibits a bias of 0.01 Sv and a random error of 0.11 Sv, which leads to a total error (0.11 Sv) that is less than 20% of the total AMOC uncertainty. The AMOC trend and its uncertainty is also not impacted by the substitution. Hence, using repeated hydrographic sections instead of moorings at these locations would lead to a more sustainable design of the RAPID array while preserving the accuracy of the AMOC estimate.

#### 4.2. Quantification of the Long-Term Additional Error of the AMOC Estimate

The total additional error of 0.11 Sv deduced from the substitution of the deep EB and MAR moorings together for A05 data informs us on the impact the substitution makes for the AMOC estimate during the limited RAPID period (2004–2020). However, as the temporal and spatial sampling of the A05 data vary from one realization to the next, and because we can expect further variations in the future, it is necessary to quantify the longer-term error in the AMOC estimate associated with the use of A05 data at these locations. We now quantify this longer-term error by assessing variations on the temporal and spatial sampling of 5-year repeated hydrographic profiles in the high-resolution model RAPID36.

We first test the effect of limited temporal sampling for the EB profile below 3,000-m depth. Figure 5a shows that the differences in the time-mean overturning streamfunctions between the 100 individual realizations and the original (i.e., without modification of the virtual array) can be up to  $\pm 0.3$  Sv at  $\sim 3,000$ -m depth. In terms of the limited spatial sampling, Figure 5b shows that the differences in the time-mean overturning streamfunctions increase as the associated spatial sampling range increases, which reflects the diminishing relationship between data at the mooring position and data farther away. To test the effect of both limited temporal and spatial sampling together, we choose a fixed spatial range of  $\Delta = 4^{\circ}$ . In this case, the uncertainty range is dominated by that for the limited spatial sampling (Figure 5c), which is slightly larger than what was found in the observations (blue lines). The mean AMOC errors in the 100 numerical realizations due to the use of the A05 data at the deep EB is 0.05 Sv for the bias and 0.10 Sv for the random error (Figure 5d).

The limited temporal and spatial sampling are now assessed when the two MAR moorings are replaced simultaneously by 5-year repeated hydrographic profiles. In terms of the limited temporal sampling, Figure 5e shows that the range of difference between the overturning streamfunctions is larger than for the EB, with differences up to  $\pm 0.9$  Sv at  $\sim 3,000$ -m depth. In terms of the limited spatial sampling, Figure 5f shows that the maximum of the differences in overturning streamfunctions is as large as for the EB, but the tendency in the differences is less uniform. To test the effect of both limited temporal and spatial sampling together, we used a fixed spatial range of  $\Delta = 1^{\circ}$ . Contrary to the EB, the uncertainty range is dominated by that for the limited temporal sampling

21699291, 2025, 11, Downloaded from https://agupubs.onlinelibrary.wiley.com/doi/10.1029/2025/C023093 by NICE, National Institute for Health and Care Excellence, Wiley Online Library on [27/11/2025]. See the

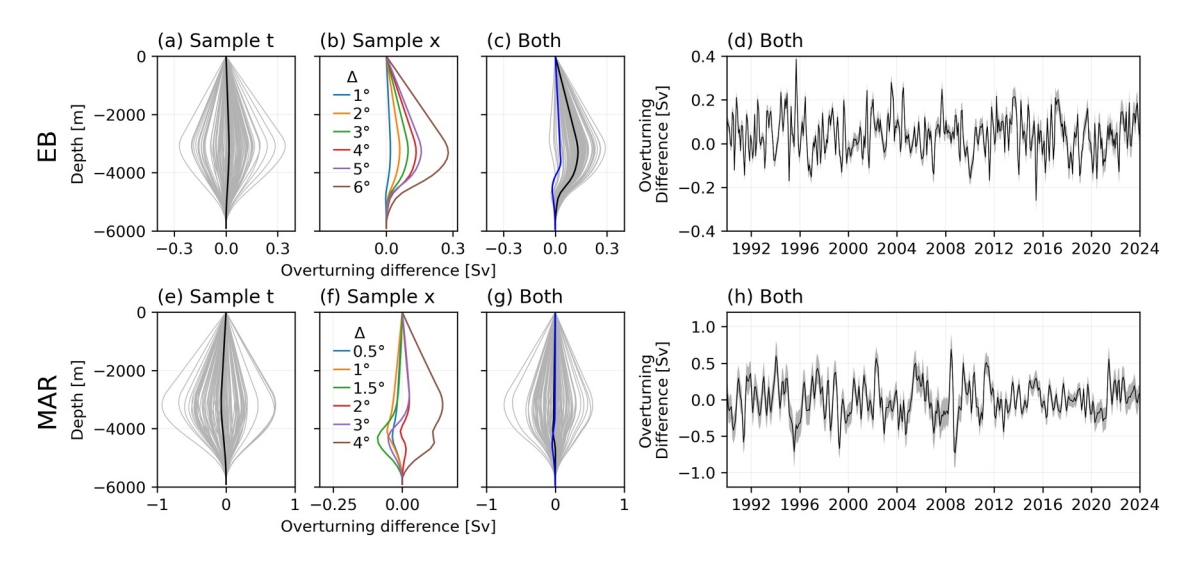


Figure 5. AMOC errors induced by variations in the temporal and spatial sampling of synoptic hydrographic sections. (a–d) Evaluation at the EB with (a) compensated overturning streamfunction differences between individual realizations and the original without replacement for limited temporal sampling only. (b) As in panel (a), but for the six realizations with limited spatial sampling only. (c) As in panel (a), but with both temporal and spatial limited sampling, using  $\Delta = 4^{\circ}$ . (d) Timeseries of AMOC differences for the experiments as in panel (c), where the black line and gray shading represent the mean and standard deviation across the 100 ensembles, respectively. (e–h) As in panels (a–d), but for the MAR using  $\Delta = 1^{\circ}$  in (g, h). In panels (a, c, e, g), thin gray lines denote individual realizations, and solid black lines denote the ensemble mean. In panels (c, g), the blue lines denote the result in observations using A05 replacements.

(Figure 5g), and the mean AMOC errors in the 100 numerical realizations due to the use of the A05 data at the MAR is larger than at the EB, which is 0.07 Sv for the bias and 0.28 Sv for the random error (Figure 5h).

Finally, when temporal and spatial limited sampling are applied to the deep EB and MAR together, the mean errors in the 100 numerical realizations is 0.08 Sv for the bias and 0.29 Sv for the random error. Figure 4b shows that the distribution of the total errors between the 100 numerical realizations of the model is close to the 20% of the total AMOC uncertainty, with the Q1–Q3 of the data at  $\sim$ 0.30 Sv. In addition, Figure 4c shows that the AMOC trend estimated from the simulated original timeseries of the model falls inside the distribution of the AMOC trend estimated from the 100 numerical realizations. The uncertainty in the AMOC trend ( $\pm$ 0.3 Sv/decade) is not modified between the 100 numerical realizations and the original timeseries of the model. As such, the modeling analysis reveals that using A05 data instead of deep moorings at the EB and MAR adds an error that does not significantly impact the long-term AMOC trend and variability.

## 5. Summary and Discussion

Motivated by the growing need of lower-cost and more sustainable AMOC observing systems while maintaining continuous, high-accuracy observations, we investigate the extent to which mooring data from the RAPID array can be replaced by data from other sources. We consider four alternative data sources to partially replace the dynamic height profiles estimated by the mooring measurements east of 76.5°W: the 5-year repeated hydrographic sections A05, the repeated hydrographic sections WBTS over the WB, the ocean reanalysis EN4 and the assimilating model GLORYS12.

We show that replacing moorings over the deep WB by any of the data sets considered results in an overestimation of the mean AMOC and a spurious trend. These large additional errors reflect particularly large variability in density below 3,000-m depth at the WB due to the variability of the deep-western boundary current, with probably eddies aliasing the boundary density of the alternative data. Similarly, significantly large AMOC errors are estimated when mooring data are replaced by alternative data over larger depth ranges at the EB. As shown by Chidichimo et al. (2010), the density in the upper 3,000 m of the EB makes an important contribution to the AMOC variability and cannot be captured by any of the other data considered here. This reveals that the three inshore moorings at the EB and the full moorings at the WB are necessary to reliably estimate the AMOC at the RAPID array.

However, replacing moorings below 3,000-m depth over the EB and MAR with data from the A05 sections does not significantly affect the estimation of the AMOC. The high-resolution model RAPID36 further shows that the additional error in the AMOC estimate due to the use of A05 data at these locations is small (0.30 Sv) and can be considered as acceptable for the AMOC estimate at the RAPID array. Hence, although the frequency of A05 observations is not sufficient to capture variability at short timescales in the deep ocean, we show that using hydrographic sections instead of moorings at these locations does not significantly impact the AMOC trend and has a negligible effect on the total uncertainty of the AMOC estimate. In comparison, whilst the EN4 and GLORYS12 data capture more temporal variability than hydrographic sections, the accuracy of the reanalysis at these locations is dependent upon the number of observations assimilated in the reanalysis, which is well constrained by observations only in the upper 2000 m and results in a significant modification of the AMOC trend. Therefore, this work reveals that the A05 data can replace the four deep moorings at the MAR and EB while continuing to reliably estimate the AMOC trend and variability at the RAPID array. These hydrographic cruises will therefore become an essential part of the observing system at 26°N, which means that the GO-SHIP and RAPID programs need to continue working closely together in the future.

At longer timescales, the high-resolution model RAPID36 highlights that the A05 data is adequate to capture the past and present AMOC trend and its uncertainty, and thus to detect long-term changes in the deep ocean volume and properties. Nevertheless, McCarthy et al. (2017) discussed the need to regularly monitor the evolution of deep volume transport across the basin to capture changes in the AMOC trend at decadal to centennial timescales. An evaluation of the suggested new design of the array in future scenarios of coupled models at high resolution is beyond the scope of this study, but a follow-up study will evaluate the extent to which the A05 repeated sections can detect future AMOC decline.

Finally, we are confident that using the A05 sections instead of moorings at these locations and depths does not significantly impact the meridional heat and freshwater transports estimated at RAPID, the changes in circulation and property at depth contributing little to these transports as compared to their changes at surface. Of importance for climate variability (Johns et al., 2023; Smeed et al., 2018), interest in direct observations of AMOC, meridional heat transport, and freshwater transport has been growing in the scientific community during the past decade, driven by a need to better understand our changing climate. Diverse observing systems have been deployed across the Atlantic to monitor these changes and inform the development of climate models (McCarthy et al., 2020), which highlighted the immense value of direct observations (Lozier, 2023; Srokosz & Bryden, 2015) but have also raised questions on their sustainability and cost going into the future. It is now a joint effort to collectively address these questions and optimize observing systems to continue measuring these key variables with the same level of accuracy.

## **Conflict of Interest**

The authors declare no conflicts of interest relevant to this study.

#### **Data Availability Statement**

The 2004–2020 RAPID AMOC timeseries are available at <a href="https://rapid.ac.uk/data/data-download">https://rapid.ac.uk/data/data-download</a> (Moat et al., 2024). The hydrographic ship survey based data set from the CLIVAR and Carbon Hydrographic Data Office (CCHDO; <a href="https://cchdo.ucsd.edu/search?q=GO-SHIP">https://cchdo.ucsd.edu/search?q=GO-SHIP</a>) and from the NOAA National Centers for Environmental Information World Ocean Database (<a href="https://www.aoml.noaa.gov/ftp/phod/pub/WBTS/Global\_Class/">https://www.aoml.noaa.gov/ftp/phod/pub/WBTS/Global\_Class/</a>) were assembled to produce the A05 and WBTS data, respectively. The model outputs used in this study are available at <a href="https://github.com/NOC-MSM/RAPID-Evolution">https://github.com/NOC-MSM/RAPID-Evolution</a> (Blaker & Harle, 2025).

## References

Atkinson, C. P., Bryden, H. L., Cunningham, S. A., & King, B. A. (2012). Atlantic transport variability at 25 N in six hydrographic sections. *Ocean Science*, 8(4), 497–523. https://doi.org/10.5194/os-8-497-2012

Balmaseda, M. A., Hernandez, F., Storto, A., Palmer, M. D., Alves, O., Shi, L., et al. (2015). The Ocean Reanalyses Intercomparison Project (ORA-IP). *Journal of Operational Oceanography*, 8(1), s80–s97. https://doi.org/10.1080/1755876X.2015.1022329

Beal, L. M., & Bryden, H. L. (1999). The velocity and vorticity structure of the Agulhas Current at 32°S. *Journal of Geophysical Research*, 104(C3), 5151–5176. https://doi.org/10.1029/1998JC900056

Bellomo, K., Angeloni, M., Corti, S., & von Hardenberg, J. (2021). Future climate change shaped by inter-model differences in Atlantic meridional overturning circulation response. *Nature Communications*, 12(1), 1–10. https://doi.org/10.1038/s41467-021-24015-w

meridional overturning circulation response. *Nature Communications*, 12(1), 1–10. https://doi.org/10.1038/s41467-021-24015-w

## Acknowledgments

TP, DS, JK, BS, AB, DR and BM are supported by Natural Environment Research Council Grants RAPID Evolution (NE/Y003551/1) and ATLANTiS (NE/Y005589/1). WJ and SE are supported by the US National Science Foundation under Grants 2148723 and 2334091. DLV and RHS are supported by the NOAA's Global Ocean Monitoring and Observing program (Grant 100007298) and by the NOAA Atlantic Oceanographic and Meteorological Laboratory. DLV was also supported by the Cooperative Institute for Marine and Atmospheric Studies (CIMAS), a cooperative institute of the University of Miami and NOAA, cooperative agreement NA20OAR4320472. We also thank the two reviewers for their helpful comments on the manuscript.

- Blaker, A., & Harle, J. (2025). NOC-MSM/RAPID-Evolution: A global double-nested NEMO configuration centred over the RAPID array latitudes (Version 1.0.2) [Dataset]. Zenodo. https://doi.org/10.5281/zenodo.14733916
- Chidichimo, M. P., Kanzow, T., Cunningham, S. A., Johns, W. E., & Marotzke, J. (2010). The contribution of eastern-boundary density variations to the Atlantic meridional overturning circulation at 26.5° N. Ocean Science, 6(2), 475–490. https://doi.org/10.5194/os-6-475-2010
- Chomiak, L. N., Yashayaev, I., Volkov, D. L., Schmid, C., & Hooper, J. A. (2022). Inferring advective timescales and overturning pathways of the Deep Western Boundary Current in the North Atlantic through Labrador Sea Water Advection. *Journal of Geophysical Research: Oceans*, 127(12), 1–23. https://doi.org/10.1029/2022JC018892
- Cunningham, S. A., Kanzow, T., Rayner, D., Baringer, M. O., Johns, W. E., Marotzke, J., et al. (2007). Temporal variability of the Atlantic meridional overturining circulation at 26.5°N. Science, 317(5840), 935–938. https://doi.org/10.1126/science.1141304
- Fox-Kemper, B., Hewitt, H. T., Xiao, C., Aðalgeirsdóttir, G., Drijfhout, S., Edwards, T., et al. (2023). Ocean, Cryosphere and Sea level change. In Climate change 2021 The physical science basis (pp. 1211–1362). Cambridge University Press. https://doi.org/10.1017/9781009157896.011
- Frajka-Williams, E., Foukal, N., & Danabasoglu, G. (2023). Should AMOC observations continue: How and why? Philosophical Transactions of the Royal Society A: Mathematical, Physical and Engineering Sciences, 381(2262), 20220195. https://doi.org/10.1098/rsta.2022.0195
- Fu, Y., Karstensen, J., & Brandt, P. (2018). Atlantic Meridional Overturning Circulation at 14.5° N in 1989 and 2013 and 24.5° N in 1992 and 2015: Volume, heat, and freshwater transports. *Ocean Science*, 14(4), 589–616. https://doi.org/10.5194/os-14-589-2018
- Good, S. A., Martin, M. J., & Rayner, N. A. (2013). EN4: Quality controlled ocean temperature and salinity profiles and monthly objective
- analyses with uncertainty estimates. *Journal of Geophysical Research: Oceans*, 118(12), 6704–6716. https://doi.org/10.1002/2013JC009067 Guiavarc'h, C., Storkey, D., Blaker, A. T., Blockley, E., Megann, A., Hewitt, H. T., et al. (2025). GOSI9: UK Global Ocean and Sea Ice configurations, *Geoscientific Model Development*, 18(2), 377–403. https://doi.org/10.5194/gmd-18-377-2025
- Hersbach, H., Bell, B., Berrisford, P., Hirahara, S., Horányi, A., Muñoz-Sabater, J., et al. (2020). The ERA5 global reanalysis. *Quarterly Journal of the Royal Meteorological Society*, 146(730), 1999–2049. https://doi.org/10.1002/qj.3803
- Jackson, L. C., Biastoch, A., Buckley, M. W., Desbruyères, D. G., Frajka-Williams, E., Moat, B., & Robson, J. (2022). The evolution of the North Atlantic Meridional Overturning Circulation since 1980. Nature Reviews Earth & Environment, 3(4), 241–254. https://doi.org/10.1038/ s43017-022-00263-2
- Johns, W. E., Baringer, M. O., Beal, L. M., Cunningham, S. A., Kanzow, T., Bryden, H. L., et al. (2011). Continuous, array-based estimates of Atlantic Ocean heat transport at 26.5°N. *Journal of Climate*, 24(10), 2429–2449. https://doi.org/10.1175/2010JCLI3997.1
- Johns, W. E., Elipot, S., Smeed, D. A., Moat, B., King, B., Volkov, D. L., & Smith, R. H. (2023). Towards two decades of Atlantic Ocean mass and heat transports at 26.5° N. *Philosophical transactions. Series A, Mathematical, physical, and engineering sciences, 381*(2262), 20220188. https://doi.org/10.1098/rsta.2022.0188
- Kanzow, T., Cunningham, S. A., Johns, W. E., Hirschi, J. J. M., Marotzke, J., Baringer, M. O., et al. (2010). Seasonal variability of the Atlantic meridional overturning circulation at 26.5°N. *Journal of Climate*, 23(21), 5678–5698. https://doi.org/10.1175/2010JCLI3389.1
- Kanzow, T., Johnson, H. L., Marshall, D. P., Cunningham, S. A., Hirschi, J. J.-M., Mujahid, A., et al. (2009). Basinwide integrated volume transports in an eddy-filled ocean. *Journal of Physical Oceanography*, 39(12), 3091–3110. https://doi.org/10.1175/2009JPO4185.1
- Lellouche, J.-M., Greiner, E., Bourdallé Badie, R., Garric, G., Melet, A., Drévillon, M., et al. (2021). The Copernicus Global 1/12° Oceanic and sea ice GLORYS12 reanalysis. Frontiers in Earth Science, 9, 698876. https://doi.org/10.3389/feart.2021.698876
- Lozier, M. S. (2023). Overturning in the subpolar North Atlantic: A review. *Philosophical Transactions of the Royal Society A: Mathematical, Physical and Engineering Sciences*, 381(2262), 20220191. https://doi.org/10.1098/rsta.2022.0191
- Lozier, M. S., Li, F., Bacon, S., Bahr, F., Bower, A. S., Cunningham, S. A., et al. (2019). A sea change in our view of overturning in the subpolar North Atlantic. *Science*, 363(6426), 516–521. https://doi.org/10.1126/science.aau6592
- Madec, G., & the NEMO System Team. (2023). NEMO ocean engine reference manual. Zenodo. https://doi.org/10.5281/zenodo.8167700
- McCarthy, G. D., Brown, P. J., Flagg, C. N., Goni, G., Houpert, L., Hughes, C. W., et al. (2020). Sustainable observations of the AMOC: Methodology and technology. *Reviews of Geophysics*, 58(1), 1–34. https://doi.org/10.1029/2019RG000654
- McCarthy, G. D., Menary, M. B., Mecking, J. V., Moat, B. I., Johns, W. E., Andrews, M. B., et al. (2017). The importance of deep, basinwide measurements in optimized Atlantic Meridional Overturning Circulation observing arrays. *Journal of Geophysical Research: Oceans*, 122(3), 1808–1826. https://doi.org/10.1002/2016JC012200
- McCarthy, G. D., Smeed, D. A., Johns, W. E., Frajka-Williams, E., Moat, B. I., Rayner, D., et al. (2015). Measuring the Atlantic meridional overturning circulation at 26°N. *Progress in Oceanography*, 130, 91–111. https://doi.org/10.1016/j.pocean.2014.10.006
- McDonagh, E. L., King, B. A., Bryden, H. L., Courtois, P., Szuts, Z., Baringer, M., et al. (2015). Continuous estimate of Atlantic Oceanic freshwater flux at 26.5°N. *Journal of Climate*, 28(22), 8888–8906. https://doi.org/10.1175/JCLI-D-14-00519.1
- Meinen, C. S., Baringer, M. O., & Garcia, R. F. (2010). Florida current transport variability: An analysis of annual and longer-period signals. *Deep Sea Research Part I: Oceanographic Research Papers*, 57(7), 835–846. https://doi.org/10.1016/j.dsr.2010.04.001
- Moat, B. I., Smeed, D. A., Rayner, D., Johns, W. E., Smith, R., Volkov, D., et al. (2024). Atlantic meridional overturning circulation observed by the RAPID-MOCHA-WBTS (RAPID-Meridional Overturning Circulation and Heatflux Array-Western Boundary Time Series) array at 26N from 2004 to 2023 (Version 2023.1) [Dataset]. British Oceanographic Data Centre - Natural Environment Research Council. https://doi.org/ 10.5285/223b34a3-2dc5-c945-e063-7086abc0f274
- Sinha, B., Smeed, D. A., McCarthy, G., Moat, B. I., Josey, S. A., Hirschi, J. J. M., et al. (2018). The accuracy of estimates of the overturning circulation from basin-wide mooring arrays. *Progress in Oceanography*, 160, 101–123. https://doi.org/10.1016/j.pocean.2017.12.001
- Smeed, D. A., Josey, S. A., Beaulieu, C., Johns, W. E., Moat, B. I., Frajka-Williams, E., et al. (2018). The North Atlantic Ocean is in a State of reduced overturning. Geophysical Research Letters, 45(3), 1527–1533. https://doi.org/10.1002/2017GL076350
- Srokosz, M. A., & Bryden, H. L. (2015). Observing the Atlantic Meridional Overturning Circulation yields a decade of inevitable surprises. Science, 348(6241), 1255575. https://doi.org/10.1126/science.1255575
- Talley, L. D. (2003). Shallow, intermediate, and deep overturning components of the global heat budget. *Journal of Physical Oceanography*, 33(3), 530–560. https://doi.org/10.1175/1520-0485(2003)033<0530:SIADOC>2.0.CO;2
- Tooth, O. J., Foukal, N. P., Johns, W. E., Johnson, H. L., & Wilson, C. (2024). Lagrangian decomposition of the AtlanticOcean heat transport at 26.5°N. *Geophysical Research Letters*, 51(14), e2023GL107399. https://doi.org/10.1029/2023GL107399
- Tsujino, H., Urakawa, S., Nakano, H., Small, R. J., Kim, W. M., Yeager, S. G., et al. (2018). JRA-55 based surface dataset for driving ocean–seaice models (JRA55-do). *Ocean Modelling*, 130, 79–139. https://doi.org/10.1016/j.ocemod.2018.07.002
- Vancoppenolle, M., Rousset, C., Blockley, E., Aksenov, Y., Feltham, D., Fichefet, T., et al. (2023). S13, the NEMO Sea Ice Engine (4.2release\_doc1.0). Zenodo. https://doi.org/10.5281/zenodo.7534900
- Volkov, D. L., Smith, R. H., Garcia, R. F., Smeed, D. A., Moat, B. I., Johns, W. E., & Baringer, M. O. (2024). Florida current transport observations reveal four decades of steady state. *Nature Communications*, 15(1), 7780. https://doi.org/10.1038/s41467-024-51879-5



## **Journal of Geophysical Research: Oceans**

10.1029/2025JC023093

Zhang, R., Sutton, R., Danabasoglu, G., Kwon, Y., Marsh, R., Yeager, S. G., et al. (2019). A review of the role of the Atlantic meridional overturning circulation in Atlantic multidecadal variability and associated climate impacts. *Reviews of Geophysics*, 57(2), 316–375. https://doi.org/10.1029/2019RG000644

Zhao, J., & Johns, W. (2014). Wind-forced interannual variability of the Atlantic Meridional Overturning Circulation at 26.5°N. *Journal of Geophysical Research: Oceans*, 119(4), 2403–2419. https://doi.org/10.1002/2013JC009407

PETIT ET AL. 14 of 14